Broadband Least-Squares Wave-Equation Migration

Shaoping Lu, Xiang Li, A.A. Valenciano, Nizar Chemingui (PGS) and Cheng Cheng (UC-Berkeley)*

Summary

In general, Least-Squares Migration (LSM) can produce images corrected for overburden effects, variations in illumination, and incomplete acquisition geometry. The modeling engine of our LSM implementation consists of a visco-acoustic anisotropic one-way wave-equation extrapolator. It has the advantage of efficiently propagating high-frequency seismic data using high-resolution earth models (e.g. derived from Full Waveform Inversion). Applications to synthetic and field data examples (from the Gulf of Mexico and the North Sea) consistently delivered higher resolution images with better amplitude balance when compared to standard seismic migration.

Introduction

Depth migration produces a blurred representation of the earth reflectivity, with biased illumination and limited wavenumber content. The image resolution at a given depth is controlled by the migration operators, the acquisition parameters (source signature, frequency bandwidth, acquisition geometry), and the earth properties at the reflector depth and the overburden (velocity, attenuation). Some of these conditions can be mitigated during acquisition and processing by employing technologies like: multi-sensor data, full azimuth acquisition geometries, deghosting, attenuation compensation and using high-resolution earth models during depth migration (i.e. models derived from Full Waveform Inversion). However, when heterogeneities are present in the earth and the acquisition geometry leads to insufficient source and receiver coverage on the surface, both the illumination and wavenumber content of the depth-migrated images can be significantly restricted.

The resolution of the depth images can be improved by posing the imaging problem in terms of least squares inversion. The Least-Squares Migration (LSM) solutions (Schuster, 1993; Nemeth et al., 1999; Prucha and Biondi, 2002) are designed to produce images of the subsurface corrected for wavefield distortions caused by acquisition and propagation effects. They implicitly solve for the earth reflectivity by means of data residual reduction in an iterative fashion, which usually demands intensive computation. In seismic exploration framework, Nemeth et al. (1999) derived a Least-Squares Migration following a high-frequency Kirchhoff integral asymptotic approximation (ray-based). Later, Prucha and Biondi (2002) derived less restrictive broadband wave equation solutions. The advantage of broadband wave-equation extrapolators is that they make better use of the high-resolution earth models derived with advanced processing technologies such as Full Waveform Inversion – FWI (Korsmo et al., 2017).

Here, we implement an LSM using an accurate visco-acoustic anisotropic one-way wave-equation operator (Valenciano et al., 2011). Our application integrates the one-way operator with a fast linear inversion solver in an efficient migration/demigration workflow, namely a Least-Squares one-way Wave-Equation Migration (LS-WEM). Applications of LS-WEM to both synthetic and field data examples improve images amplitude balance and enhance both temporal and spatial resolution.

Methodology

Seismic migration is the adjoint solution to the forward modeling problem:

$$\boldsymbol{m} = \boldsymbol{L}^{T} \boldsymbol{d}_{obs} \qquad (1)$$

where, $\boldsymbol{d}_{obs}$ is the observed data , $\boldsymbol{L}$ represents the linearized (Born) modeling operator, and its adjoint $\boldsymbol{L}^{T}$ is the migration operator. However, the heterogeneity of the overburden and/or limitations of the acquisition geometry can affect the illumination and wavenumber content of the estimated image $\boldsymbol{m}$.

A better approximation of the earth reflectivity is obtained by using a least squares inversion, which solves a minimization problem to approximate the true reflectivity $\boldsymbol{m}$ as:

$$\boldsymbol{m} = \boldsymbol{argmin}_{m} \frac{1}{2} \| \boldsymbol{d}_{obs} - \boldsymbol{L}\boldsymbol{m} \|_{2}^{2} \qquad (2)$$

In this case, the acquisition geometry, which relates to the operator $\boldsymbol{L}$, has less effect to the resulting image $\boldsymbol{m}$.

Here we introduce an implicit method to solve the Least-Squares problem. The LSM simulates data by wave-equation Born modeling, and iteratively updates the reflectivity by migration of the misfits between the observed and simulated data. The algorithm can be summarized by the diagram in Figure 1 using an iterative modeling/migration framework. The first step of the flow is to produce an approximate reflectivity (migration). In the next step, the reflectivity is used in Born modeling. When the data residual $\| \boldsymbol{d}_{obs} - \boldsymbol{d}_{mod} \|$ is large, it is migrated to update the image $\boldsymbol{m}$. The inversion converges when the simulated data matches the observation. One iteration (blue loop in Figure 1) comprises one Born modeling and one migration.

The computational cost of the iterative LSM relies on the efficiency of the wavefield propagation algorithm. Here, we implement the inversion using a one-way wave-equation operator (Valenciano et al., 2011), which has advantages of both accuracy and efficiency. In addition, our implementation combines the one-way extrapolator with fast linear inversion solvers into an efficient migration inversion system.

Synthetic and field data examples

We have applied LS-WEM to the 2D Sigsbee2b synthetic model [Figure 2]. The migration result [Figure 2A] shows uneven illumination from left sedimentary to subsalt area, including shadow zones related to the complex salt structures. LS-WEM improves the illumination by balancing the image amplitudes and reducing the effects of the shadow zones [Figure 2B]. LS-WEM also enhances temporal resolution by broadening the frequency spectrum [Figure 2E]. Figure 2C and 2D show that LS-WEM balances the wavenumber content and improves the image of the faults and dipping salt flacks (indicated by arrows).

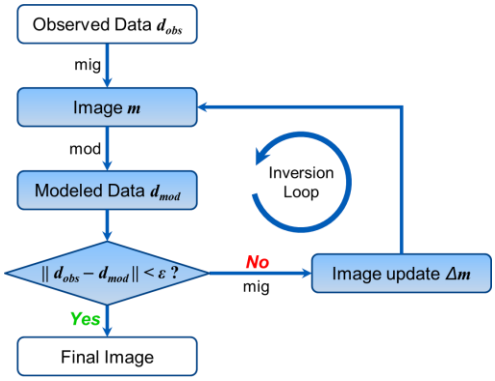

Figure 1: *An iterative LSM algorithm solves for the earth reflectivity* $\mathbf{m}$*. It simulates synthetic data* $\mathbf{d}_{mod}$ *by using a Born modeling operator, and iteratively update the reflectivity image* $\mathbf{m}$ *using migration of the data residual* $\|\mathbf{d}_{obs} - \mathbf{d}_{mod}\|$.

In addition, LS-WEM converges rapidly to the true solution, reducing the data residuals by 90% in only four iterations [Figure 2F].

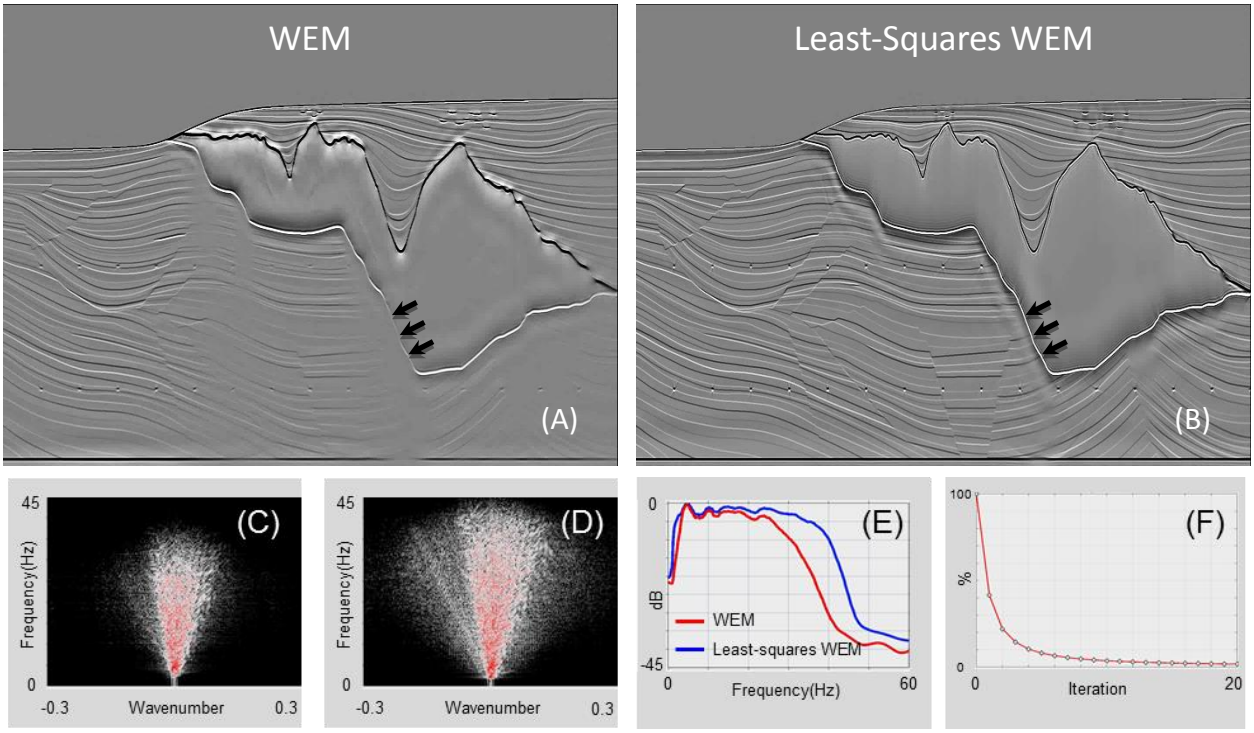

Figure 2*: Sigsbee2b 2D synthetic example: (A) WEM image; (B) LS-WEM image; (C) F-K spectrum of WEM; (D) F-K spectrum of LS-WEM; (E) Frequency spectra of WEM [red] and LS-WEM [blue]; (F) LS-WEM objective function convergence rate.*

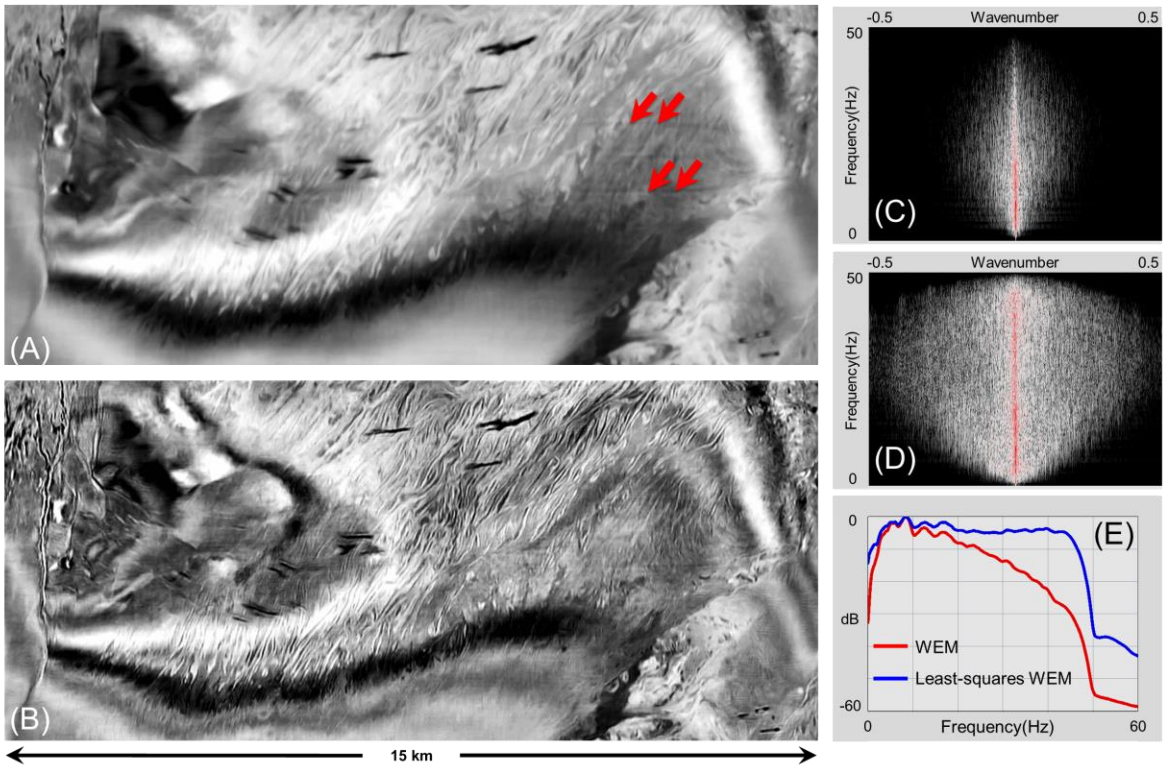

***Figure 3**: Gulf of Mexico 3D WAZ field data example: (A) Depth slice at 1150m from WEM; (B) Depth slice at 1150m from LS-WEM; (C) WEM F-K spectrum; (D) LS-WEM F-K spectrum; (E) Frequency spectra of WEM and LS-WEM.*

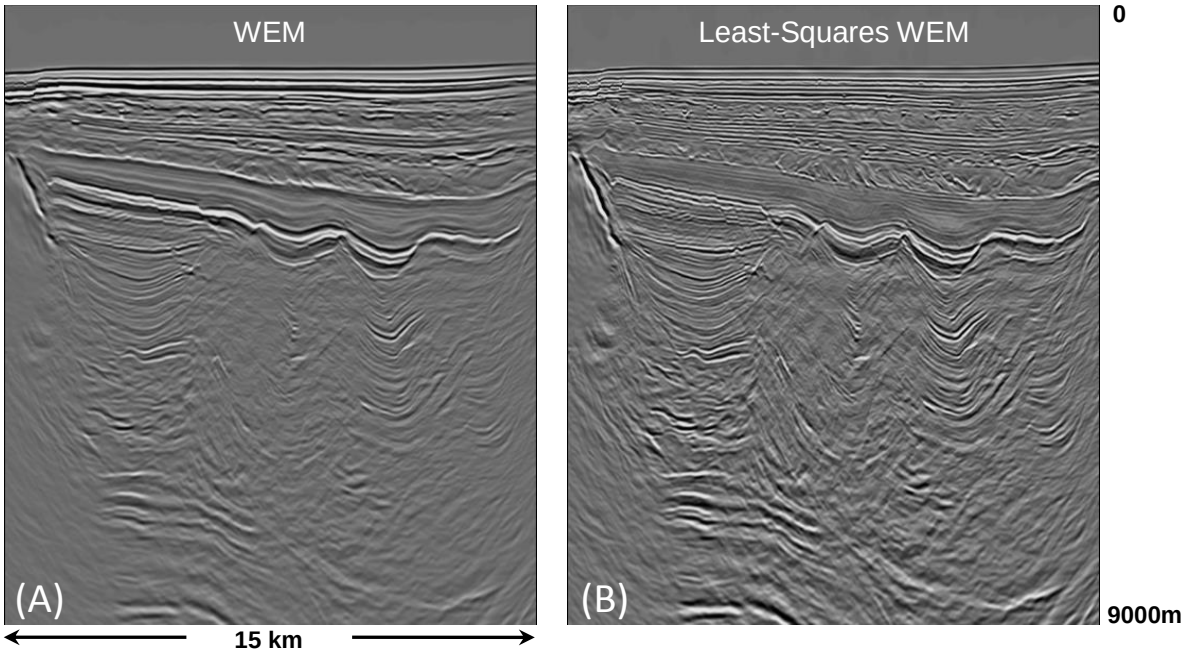

***Figure 4**: Gulf of Mexico 3D WAZ field data example: Inline and xline images from (A) WEM and (**B**) LS-WEM.*

We also applied the LS-WEM to a wide azimuth (WAZ) data from the Gulf of Mexico. The results also demonstrate that LS-WEM can deliver superior images compared to the standard migration [Figure 3 and 4].

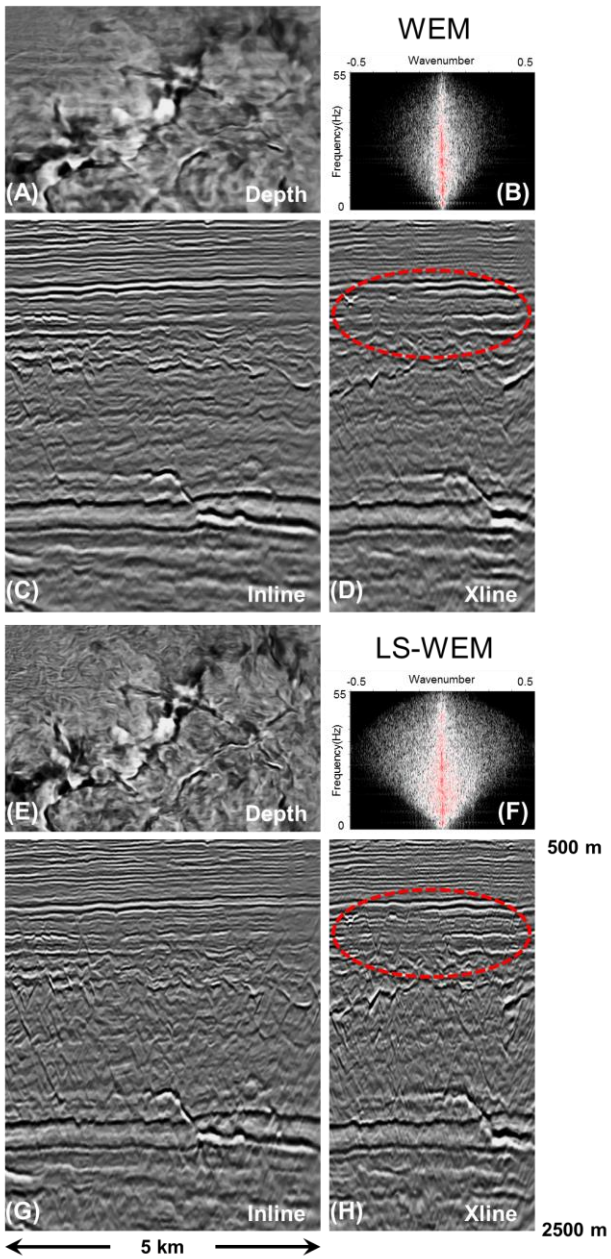

Figure 5: *North Sea 3D NAZ field data example. Top: WEM results; Bottom: LS-WEM results. The depth slice is at 1.8km.*

The image improvements of LS-WEM over the standard migration can be summarized as: reduction of sail line acquisition footprint (lateral stripes indicated by arrows in Figure 3A), better resolution, and improved wavenumber content [Figure 3C, 3D and 3E]. The inline images also reveal significant improvement in spatial resolution from LS-WEM [Figure 4B]. In addition, the LS-WEM balances the overall imaging amplitude, and especially augments the deeper reflection targets. More importantly, the LS-WEM creates better images of fault structures.

Another example of 3D narrow azimuth (NAZ) data from North Sea further illustrates the advantages of applying LS-WEM to strongly attenuative media with high resolution velocity model (Korsmo et al., 2017). Figure 5 shows a comparison of the results from WEM and LS-WEM. The standard migration images are corrupted by the acquisition footprints [Figure 5A], a typical problem in a shallow water environment. The LS-WEM solution effectively reduces the acquisition footprint leading to a more interpretable image [Figure 5E]. LS-WEM also improves the resolution as being illustrated in the first two examples. The LS-WEM creates an image with much broader wavenumber contents [Figure 5F] compared to WEM [Figure 5B]. The improved high wavenumber contents make the LS-WEM solution produce a better image of the fault planes (circled) [Figure 5H].

Conclusions

We introduce an efficient iterative Least-Squares Wave-Equation Migration (LS-WEM) solution for broadband imaging. The Least-Squares Migration is implemented using a one-way wave-equation wavefield propagator, which is able to fully utilize both the broader seismic bandwidth and the high-resolution velocity information from FWI. Our implementation combines the one-way extrapolator with fast linear inversion solvers into an efficient migration inversion system. LS-WEM application to both synthetic and field data demonstrate its ability to generate high-resolution images with better balanced amplitudes, broader frequency bandwidth and larger wavenumber content.

Acknowledgements

The authors thank PGS for permission to publish this work and for the approval to show the Multi-Client Gulf of Mexico data. We are also grateful to Aker BP for permission to publish the North Sea results. Furthermore, we thank Øystein Korsmo and Grunde Rønholt for supports and valuable discussion during the North Sea project.

EDITED REFERENCES

Note: This reference list is a copyedited version of the reference list submitted by the author. Reference lists for the 2017 SEG Technical Program Expanded Abstracts have been copyedited so that references provided with the online metadata for each paper will achieve a high degree of linking to cited sources that appear on the Web.

REFERENCES

Korsmo Ø., O. J. Askim, Ø. Runde, and G. Rønholt, 2017, High fidelity velocity model building, imaging and reflectivity inversion — A case study over the Viking Graben area, Norwegian North Sea: 79th Annual International Conference and Exhibition, EAGE, Extended Abstracts, https://doi.org/10.3997/2214-4609.201700818.

Nemeth, T., C. Wu, and G. Schuster, 1999, Least-squares migration of incomplete reflection data: Geophysics, **64**, 208–221, https://doi.org/10.1190/1.1444517.

Prucha, M. and B. Biondi, 2002, Subsalt event regularization with steering filters: 72th Annual International Meeting, SEG, Expanded Abstracts, 1176-1179, https://doi.org/10.1190/1.1816859.

Schuster, G., 1993, Least-squares crosswell migration: 63rd Annual International Meeting, SEG Expanded Abstracts, 110–113, https://doi.org/10.1190/1.1822308.

Valenciano A. A., N, Chemingui, D. Whitmore, and S. Brandsberg-Dahl, 2011, Wave Equation Migration with Attenuation Compensation: 73rd Annual International Conference and Exhibition, EAGE, Extended Abstracts, 232-236, https://doi.org/10.1190/1.3627674.